

## Supporting Information for

### Dual-Cation Doping Precisely Reducing Energy Barrier of Rate-Determining Step for Promoting Oxygen-Evolving Activity

Hui Xu <sup>a,b,\*</sup>, Cheng Wang <sup>b</sup>, Bingji Huang <sup>a</sup>, Hongyuan Shang <sup>c</sup>, Yukou Du <sup>b\*</sup>

<sup>a</sup> *Key Laboratory of Advanced Catalytic Materials and Technology, Advanced Catalysis and Green Manufacturing Collaborative Innovation Center, Changzhou University, Changzhou, Jiangsu Province 213164, China*

<sup>b</sup> *College of Chemistry Chemical Engineering and Materials Science, Soochow University, Suzhou, 215123 P. R. China*

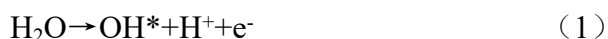
<sup>c</sup> *College of Pharmacy, Shanxi Medical University, Taiyuan, 030001, PR China*

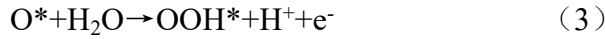
*Corresponding authors: xuhui006@cczu.edu.cn (H. Xu); duyk@suda.edu.cn (Y. Du)*

#### DFT calculations

Our computational simulations were performed by Vienna ab-initio simulation package (VASP) with the projector augmented wave pseudo-potentials (PAW) to describe the interaction between atomic cores and valence electrons with density functional theory (DFT). The Perdew–Burke–Ernzerhof (PBE) functional within the generalized gradient approximation (GGA) was used to implement DFT calculations. The Co(OH)<sub>2</sub> slab model was employed to simulate the surface properties. The reasonable vacuum layers were set around 15 Å in the z-direction to avoid interaction between planes. A cutoff energy of 450 eV was provided and a 3×3×1 Monkhorst Pack k-point sampling was chosen for the well converged energy values. Geometry optimizations were pursued until the force on each atom falls below the convergence criterion of 0.05 eV/Å and energies were converged within 10<sup>-5</sup> eV.

OER steps:





Gibbs free energy can be obtained by adding corrections including entropic ( $TS$ ) and zero-point energy (ZPE) to calculated DFT energy, so that  $\Delta G = \Delta E_{\text{DFT}} + \Delta \text{ZPE} - T\Delta S - eU$  (5)

where the  $E_{\text{DFT}}$  is the calculated DFT reaction energy,  $\Delta \text{ZPE}$  is the change in ZPE calculated from the vibrational frequencies and  $\Delta S$  is the change in the entropy referring to thermodynamics databases. The electrode potential is adopted with respect to the reversible hydrogen electrode, which makes the standard electrochemical potential of electron involved in reaction ( $G_e$ ) equal to  $-eU$ , and the standard electrochemical potential of the proton ( $G_{\text{H}^+}$ ) equal to that of the hydrogen atom in gaseous  $\text{H}_2$  ( $1/2G_{\text{H}_2}$ ). Considering that the triplet state of the  $\text{O}_2$  molecule is poorly described in the current DFT scheme, the free energy of the  $\text{O}_2$  molecule was derived according to  $G_{\text{O}_2} = 2G_{\text{H}_2\text{O}} - 2G_{\text{H}_2} + 4.92$ .

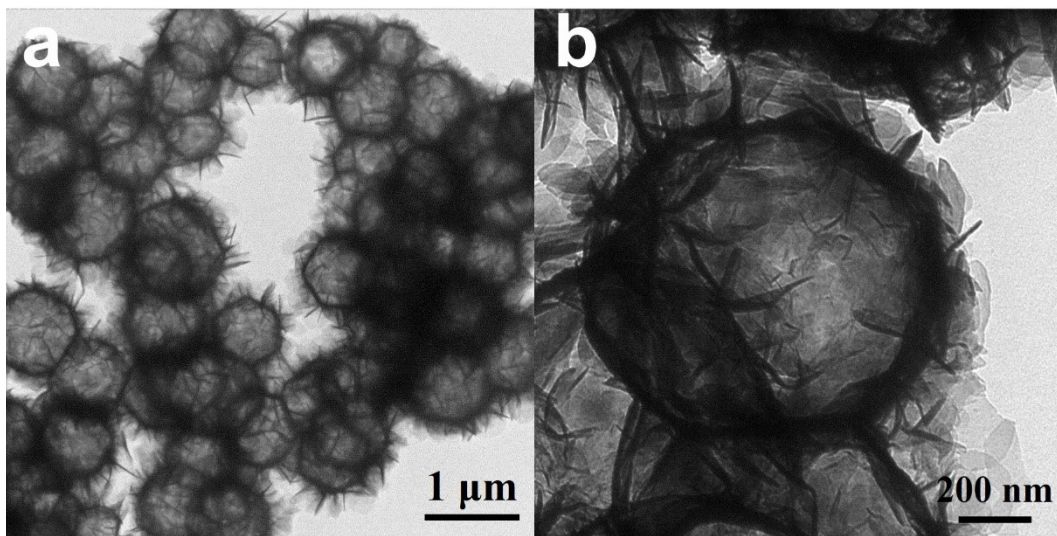


**Fig.S1** Representative TEM images of the Fe-doped  $\text{Co}(\text{OH})_2$  open sunflowers.

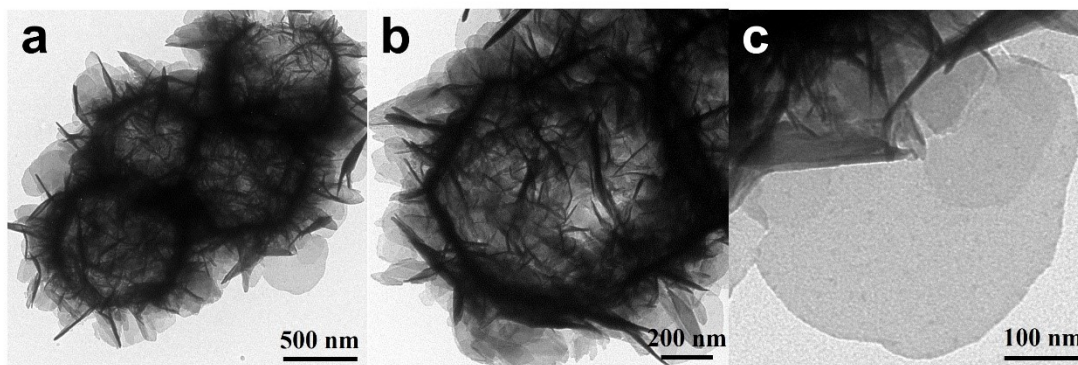


**Fig.S2** Representative TEM images of the Ir, Fe-codoped  $\text{Co(OH)}_2$  open sunflowers.

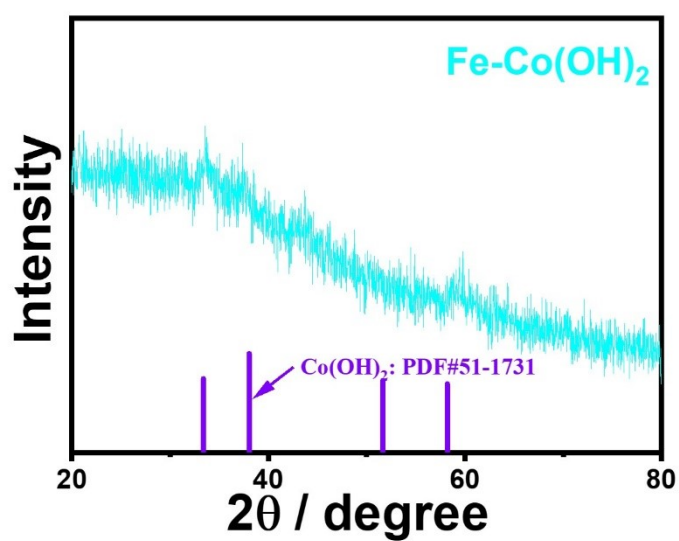


**Fig.S3** XRD pattern of the Fe-doped  $\text{Co(OH)}_2$  open sunflowers.

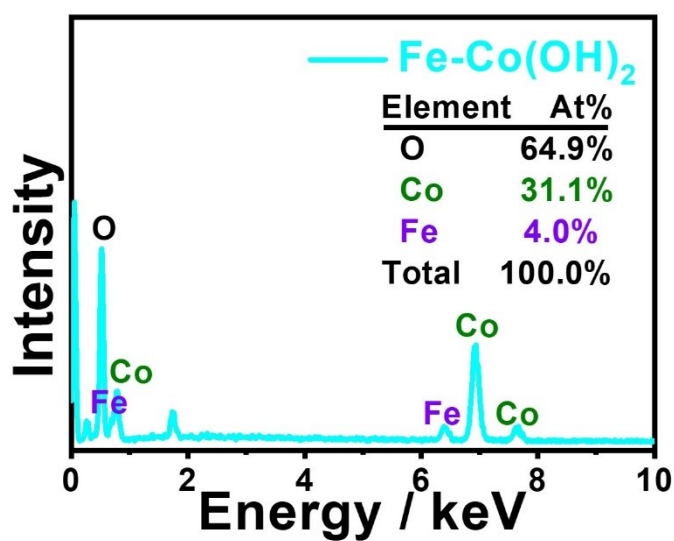


**Fig.S4** EDX spectrum of the Fe-doped  $\text{Co}(\text{OH})_2$  open sunflowers.

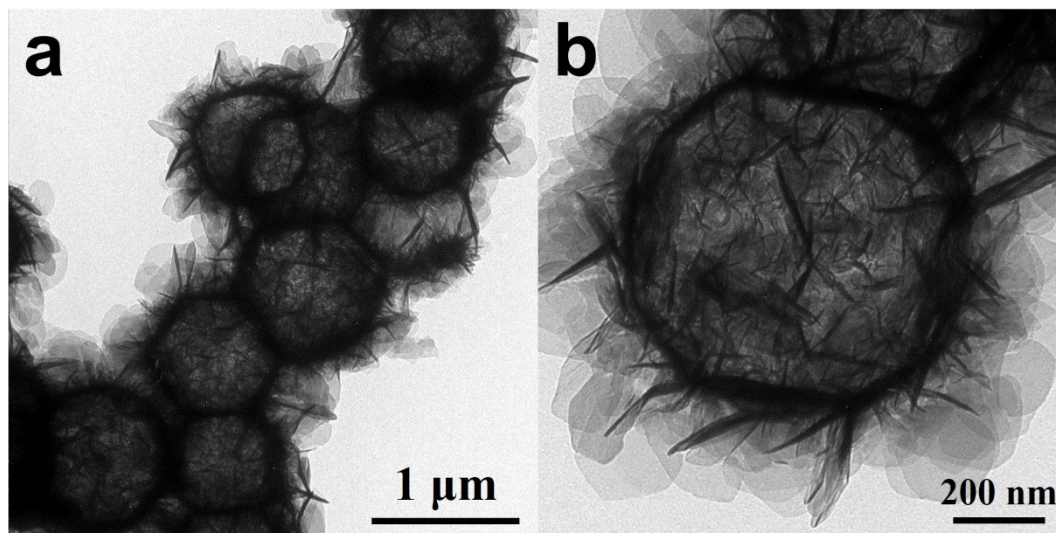


**Fig.S5** Additional TEM images of the Ru, Fe-codoped  $\text{Co}(\text{OH})_2$  open sunflowers.

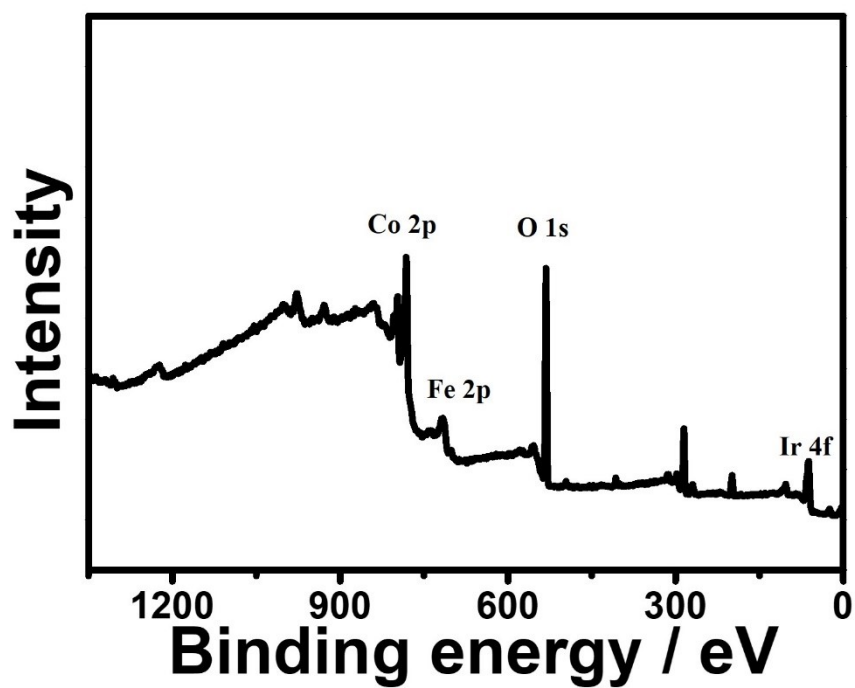


**Fig.S6** XPS survey spectrum of the Ir, Fe- $\text{Co}(\text{OH})_2$  open sunflowers.

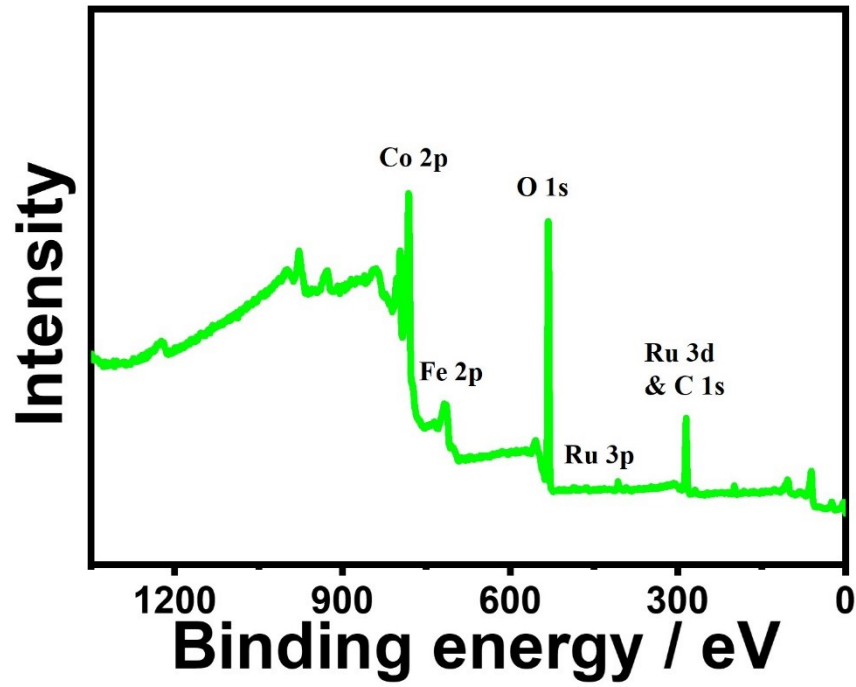


Fig.S7 XPS survey spectrum of the Ru, Fe-Co(OH)<sub>2</sub> open sunflowers.

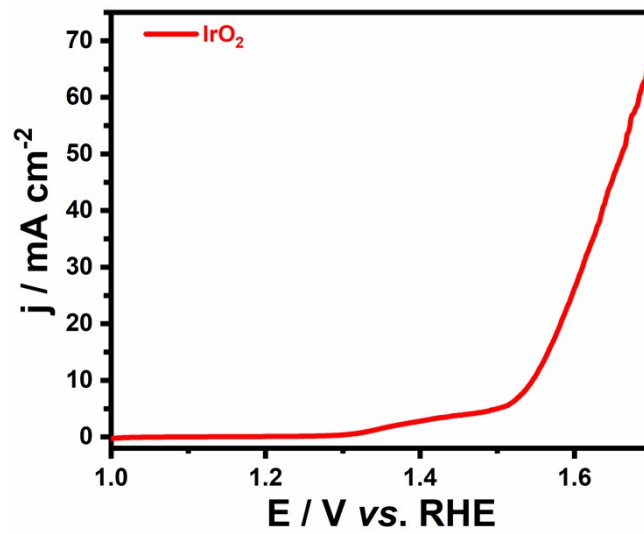
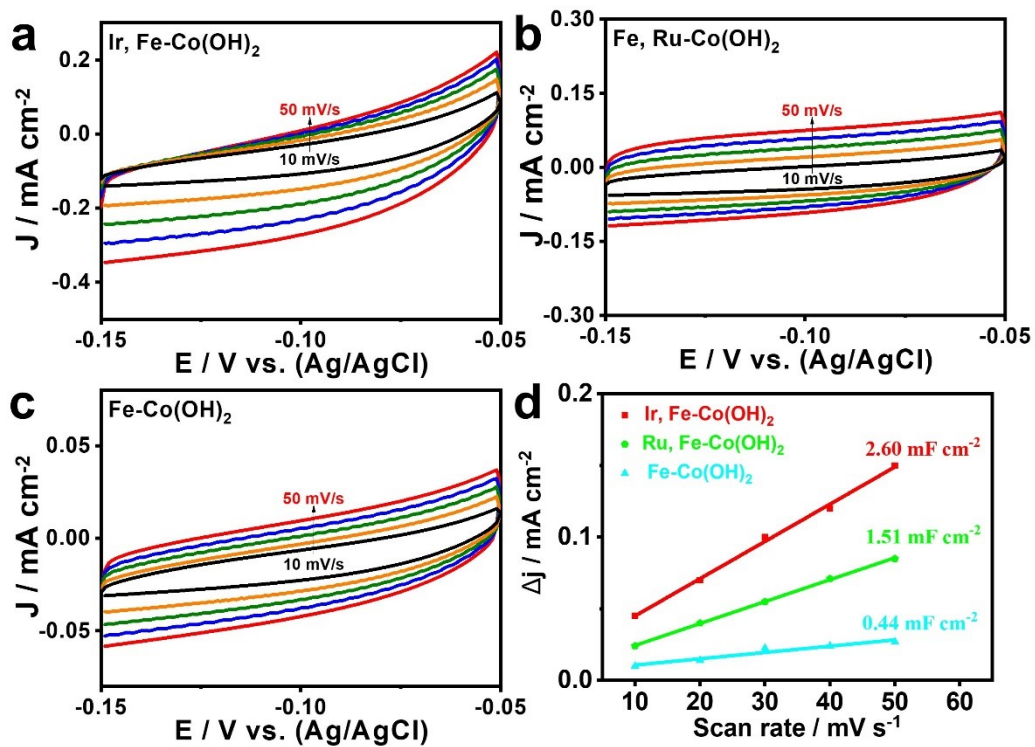
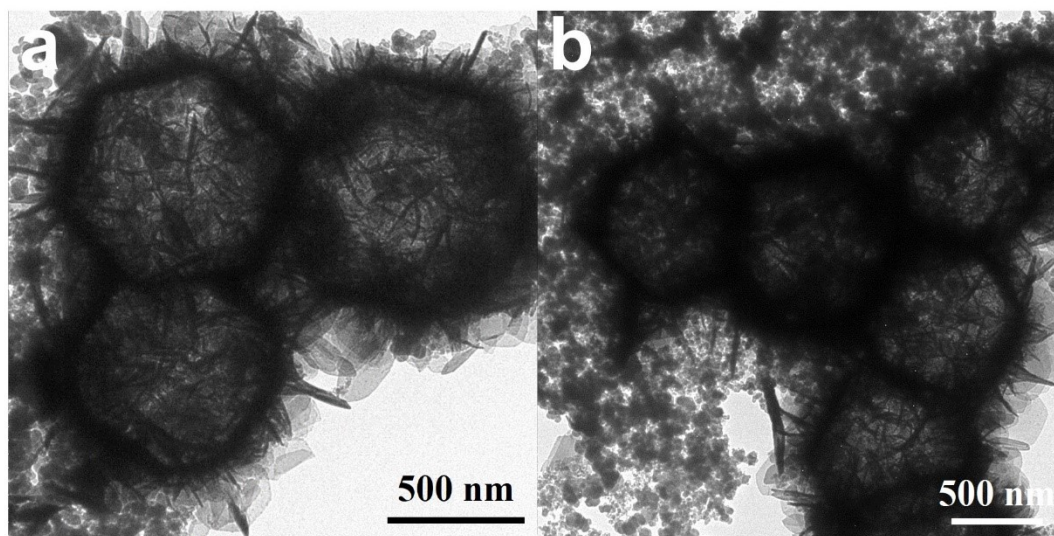


Fig.S8 LSV polarization curve of IrO<sub>2</sub> towards OER in 1 M KOH solution.



**Fig.S9** CV curves of (a) Ir, Fe-Co(OH)<sub>2</sub>, (b) Ru, Fe-Co(OH)<sub>2</sub>, and (c) Fe-Co(OH)<sub>2</sub> at different scan rates. (d) The corresponding linear fitting of the current density versus scan rates.



**Fig.S10** TEM images of the conductive carbon supported Ir, Fe-Co(OH)<sub>2</sub>.

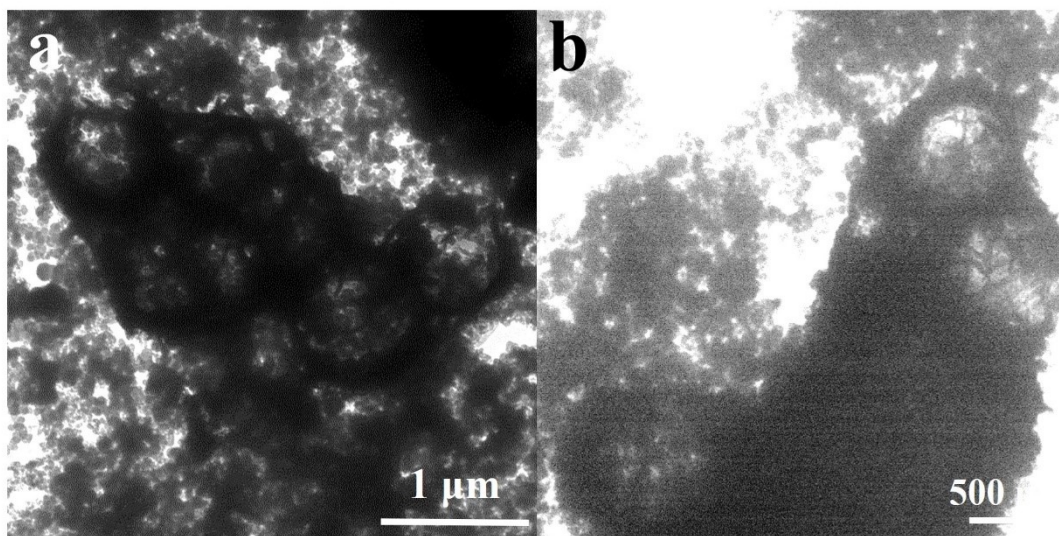


**Fig.S11** TEM images of the conductive carbon supported Ir, Fe-Co(OH)<sub>2</sub> after long-time electrochemical operation.

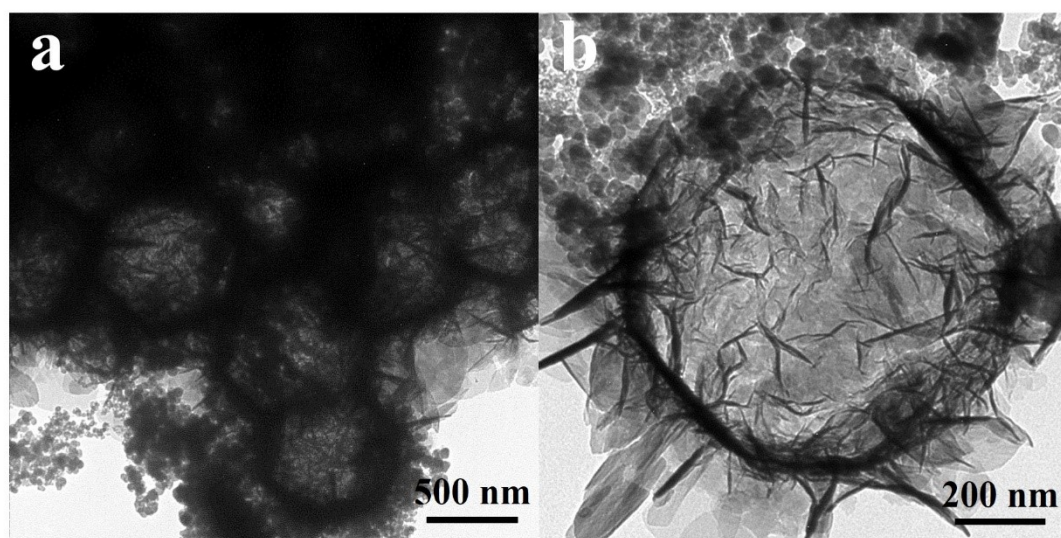


**Fig.S12** TEM images of the conductive carbon supported Ru, Fe-Co(OH)<sub>2</sub>.

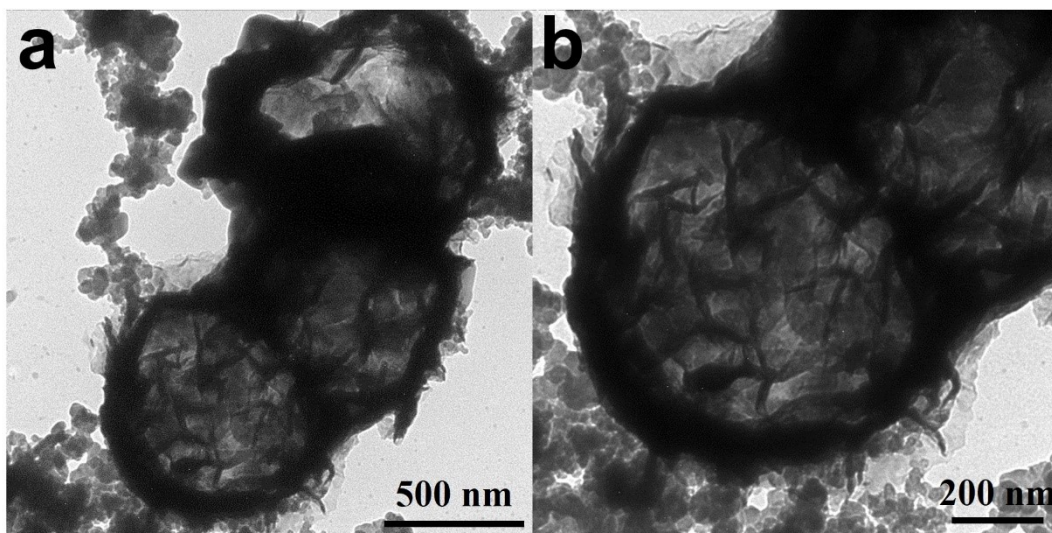


**Fig.S13** TEM images of the conductive carbon supported Ir, Fe-Co(OH)<sub>2</sub> after long-time electrochemical operation.

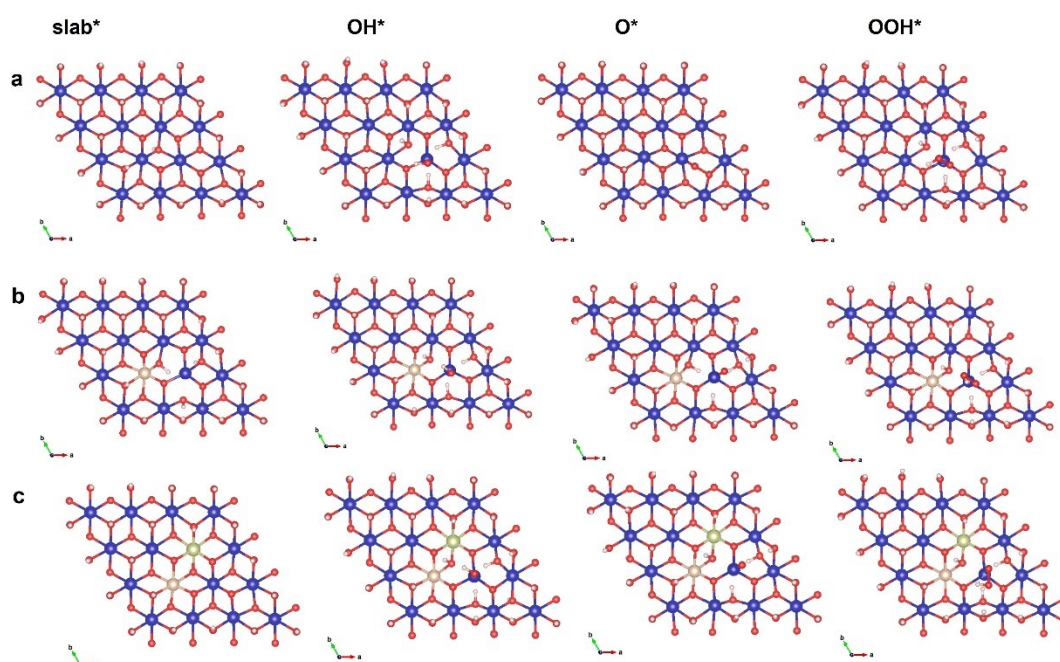


**Fig.S14** Simulation model for the active species of (a) Co(OH)<sub>2</sub>, (b) Fe-Co(OH)<sub>2</sub>, and (c) Ir, Fe-Co(OH)<sub>2</sub>. The blue, red, brown, yellow, and white represent Co, O, Fe, Ir, and H, respectively.

**Table S1** Summary of the cell voltage of two-electrode water electrolysis.

Catalysts	Electrolyte	V@10 mA cm <sup>-2</sup>	Reference
CoMoOS-100/NF//Pt/C/NF	1 M KOH	1.58	[1]
(Ru-Co)O <sub>x</sub> //Pt/C	1 M KOH	1.57	[2]
CoMoRuO <sub>x</sub> -350//Pt/C	1 M KOH	1.55	[3]
RuTe <sub>2</sub> //RuTe <sub>2</sub>	1 M KOH	1.57	[4]
Ni/Ni <sub>8</sub> P <sub>3</sub> //Ni/Ni <sub>8</sub> P <sub>3</sub>	1 M KOH	1.61	[5]
Ru-NiCo MOF//Pt/C	1 M KOH	1.57	[6]
Ru@CoFe/D-MOFs//Pt/C	1 M KOH	1.56	[7]
IrO <sub>2</sub> //Pt/C	1 M KOH	1.58	[8]
<b>Ir, Fe-Co(OH)<sub>2</sub>//Pt/C</b>	1 M KOH	<b>1.55</b>	<b>This work</b>

**Table S2** Summary of the d-band center of Co(OH)<sub>2</sub>, Fe-Co(OH)<sub>2</sub>, and Ir, Fe-Co(OH)<sub>2</sub>.

Catalysts	d-Band-Center (UP)	d-Band-Center (Down)	d-Band-Center (Average)
Co(OH) <sub>2</sub>	-2.3525	-0.2310	-1.2963
Fe-Co(OH) <sub>2</sub>	-3.5030	0.6776	-1.4356
Ir, Fe-Co(OH) <sub>2</sub>	-3.7392	0.4497	-1.6682

## References

- [1] H. Xu, H. Shang, C. Wang, L. Jin, C. Chen, C. Wang, Y. Du, Three-dimensional open CoMoO<sub>x</sub>/CoMoS<sub>x</sub>/CoS<sub>x</sub> nanobox electrocatalysts for efficient oxygen evolution reaction, *Applied Catalysis B: Environmental*, 265 (2020).
- [2] C. Wang, H. Shang, J. Li, Y. Wang, H. Xu, C. Wang, J. Guo, Y. Du, Ultralow Ru doping induced interface engineering in MOF derived ruthenium-cobalt oxide hollow nanobox for efficient water oxidation electrocatalysis, *Chemical Engineering Journal*, 420 (2021).
- [3] C. Wang, H. Shang, Y. Wang, H. Xu, J. Li, Y. Du, Interfacial electronic structure modulation enables CoMoO<sub>x</sub>/CoO<sub>x</sub>/RuO<sub>x</sub> to boost advanced oxygen evolution electrocatalysis, *Journal of Materials Chemistry A*, 9 (2021) 14601-14606.
- [4] B. Tang, X. Yang, Z. Kang, L. Feng, Crystallized RuTe<sub>2</sub> as unexpected bifunctional catalyst for overall water splitting, *Applied Catalysis B: Environmental*, 278 (2020).
- [5] G.F. Chen, T.Y. Ma, Z.Q. Liu, N. Li, Y.Z. Su, K. Davey, S.Z. Qiao, Efficient and Stable Bifunctional Electrocatalysts Ni/Ni<sub>x</sub>My (M = P, S) for Overall Water Splitting, *Advanced Functional Materials*, 26 (2016) 3314-3323.
- [6] D. Liu, H. Xu, C. Wang, H. Shang, R. Yu, Y. Wang, J. Li, X. Li, Y. Du, 3D Porous Ru-Doped NiCo-MOF Hollow Nanospheres for Boosting Oxygen Evolution Reaction Electrocatalysis, *Inorg Chem*, 60 (2021) 5882-5889.
- [7] D. Liu, C. Wang, Z. Zhou, C. Ye, R. Yu, C. Wang, Y. Du, Ultra-low Ru doped MOF-derived hollow nanorods for efficient oxygen evolution reaction, *Inorganic Chemistry Frontiers*, (2022).
- [8] Z. Li, D. Liu, X. Lu, M. Du, Z. Chen, J. Teng, R. Sha, L. Tian, Boosting oxygen evolution of layered double hydroxide through electronic coupling with ultralow noble metal doping, *Dalton Trans*, 51 (2022) 1527-1532.